

Oxidation and Reduction Reactions of Hydroperoxocobalt Macrocycles

Wei-Dong Wang, Andreja Bakac,* and James H. Espenson*

Department of Chemistry and the Ames Laboratory, Iowa State University, Ames, Iowa 50011

Received January 26, 1995[⊗]

The reduction of LCoOOH^{2+} ($\text{L} = \text{L}^1 = [14]\text{janeN}_4$ and $\text{L}^2 = \text{Me}_6[14]\text{janeN}_4$) by Cr^{2+} , Fe^{2+} , VO^{2+} , V^{2+} , Ti^{3+} , and $\text{Co}(\text{tm})^{2+}$ has been studied in acidic aqueous solution. The $\text{L}^1\text{CoOOH}^{2+}/\text{Fe}^{2+}$ reaction takes place with a second-order rate constant $4.8 \text{ L mol}^{-1} \text{ s}^{-1}$ at 25°C and $0.10 \text{ M H}_3\text{O}^+$. It is accompanied by a large negative entropy of activation, $-122 \text{ J mol}^{-1} \text{ K}^{-1}$. In the presence of a large excess of Fe^{2+} , this reaction proceeds with a 1:2 stoichiometry and produces L^1Co^{3+} and Fe^{3+} . A Fenton mechanism is proposed for this and other reduction reactions of LCoOOH^{2+} . The oxidation of LCoOOH^{2+} by $\text{Ru}(\text{bipy})_3^{3+}$, $\text{Fe}(\text{phen})_3^{3+}$, IrCl_6^{2-} , VO_2^+ , and Fe^{3+} has also been investigated. The outer-sphere electron transfer reactions with $\text{Ru}(\text{bipy})_3^{3+}$, $\text{Fe}(\text{phen})_3^{3+}$, and IrCl_6^{2-} proceed with a 1:2 stoichiometry. The reaction of $\text{L}^1\text{CoOOH}^{2+}$ with Fe^{3+} produces O_2 with a second-order rate constant $2.74 \text{ L mol}^{-1} \text{ s}^{-1}$ at 25°C and $0.10 \text{ M H}_3\text{O}^+$. Unlike the reduction reactions, the kinetics of the oxidation of $\text{L}^1\text{CoOOH}^{2+}$ are acid-dependent.

Introduction

Reactions of hydrogen peroxide,¹ organic hydroperoxides,² and complexes of transition metals with the hydroperoxide anion³ continue to be of interest. Our particular focus has been the reduction of these species by transition metal complexes. On the basis of kinetic data and other supporting evidence, it is

now clear that coordination of one of the peroxide oxygens to the metal reductant in the transition state is required.

In general, two mechanisms have been formulated to account for the observations. One is the Fenton mechanism,⁴ a single-electron process that produces HO^\bullet from H_2O_2 , RO^\bullet from ROOH , and $(\text{H}_2\text{O})_5\text{CrO}^{2+}$ from $(\text{H}_2\text{O})_5\text{CrOOH}^{2+}$, this being the only hydroperoxo-metal complex examined to date. An alternative mechanism is comprised of a two-electron event,^{5,6} and we term it the oxo mechanism. For the same examples, the intermediate in all three instances is the metal-oxo species $\text{LM}^{\text{IV}}\text{O}$ if LM^{II} represents the reducing agent. The balance between the two mechanisms appears to be rather delicately poised. Changes in the solvent,⁵ the metal reductants,⁶ or the secondary ligands of the metal reductants suffice to alter the mechanism.

Previous quantitative work has been limited to $(\text{H}_2\text{O})_5\text{CrOOH}^{2+}$, for which the data suggested a Fenton mechanism.^{31,m} There it proved possible to validate the intermediacy of the oxochromium(IV) ion, $(\text{H}_2\text{O})_5\text{CrO}^{2+}$, a species well established earlier.⁷ We have now chosen to work with the hydroperoxo complexes of cobalt macrocycles ($[14]\text{janeN}_4$) $\text{Co}(\text{OH}_2)\text{OOH}^{2+}$, abbreviated $\text{L}^1\text{CoOOH}^{2+}$, a species that has been well characterized in the literature,^{3e,8} and $(\text{Me}_6[14]\text{janeN}_4)\text{Co}(\text{OH}_2)\text{OOH}^{2+}$, abbreviated $\text{L}^2\text{CoOOH}^{2+}$.

The issues that the cobalt hydroperoxide complexes present can be appreciated by making reference to Scheme 1. This diagram presents the first step of a generalized reaction with the reductant M^{2+} , the reaction being considered to proceed by each of the alternative mechanisms. (In each, the necessary protons are to be supplied at acidic pH's to convert hydroxo to aqua ligands.) The scheme also shows for each alternative the second rapid step that is needed to complete the net reaction. As one can see, with LCoOOH^{2+} ($\text{L} = \text{L}^1$ or L^2) as the reactant, the reaction chooses its mechanism between alternatives (if indeed these are the only two) that feature seemingly high-energy intermediates. They are oxocobalt(IV) or another oxometal complex, $\text{M}^{\text{IV}}\text{O}^{2+}$, such as oxoiron(IV) when $\text{Fe}(\text{H}_2\text{O})_6^{2+}$ is the reductant.

[⊗] Abstract published in *Advance ACS Abstracts*, July 1, 1995.

- (1) (a) *Catalytic Oxidations with Hydrogen Peroxide as Oxidant*; Strukul, G., Ed.; Kluwer Academic: Boston, MA, 1992. (b) Heckman, R. A.; Espenson, J. H. *Inorg. Chem.* **1979**, *18*, 38. (c) Bakac, A.; Espenson, J. H. *Inorg. Chem.* **1983**, *22*, 779. (d) Bakac, A.; Espenson, J. H. *J. Am. Chem. Soc.* **1986**, *108*, 713. (e) Rahhal, S.; Richter, H. W. *J. Am. Chem. Soc.* **1988**, *110*, 3126. (f) Masarwa, M.; Cohen, H.; Meyerstein, D.; Hickman, D. L.; Bakac, A.; Espenson, J. H. *J. Am. Chem. Soc.* **1988**, *110*, 4293. (g) Sadler, N.; Scott, S. L.; Bakac, A.; Espenson, J. H.; Ram, M. S. *Inorg. Chem.* **1989**, *28*, 3951. (h) Sharma, V. K.; Bielski, B. H. *J. Inorg. Chem.* **1991**, *30*, 4306. (i) Sawyer, D. T.; Kang, C.; Llobet, A.; Redman, C. J. *J. Am. Chem. Soc.* **1993**, *115*, 5817. (j) Goldstein, S.; Meyerstein, D.; Czapski, G. *Free Rad. Biol. Med.* **1993**, *15*, 435. (k) Wink, D. A.; Nims, R. W.; Saavedra, J. E.; Utermahlen, W. E. Jr.; Ford, P. C. *Proc. Natl. Acad. Sci. U.S.A.* **1994**, *91*, 6604.
- (2) (a) *The Chemistry of Peroxides*; Patai, S., Ed.; Wiley: New York, 1983. (b) *Organic Peroxygen Chemistry*; Herrmann, W. A., Ed.; Topics in Current Chemistry 164, Springer-Verlag: New York, 1993. (c) *Organic Peroxides*; Ando, W., Ed.; Wiley: New York, 1992. (d) Hyde, M. R.; Espenson, J. H. *J. Am. Chem. Soc.* **1976**, *98*, 4463. (e) Espenson, J. H.; Martin, A. H. *J. Am. Chem. Soc.* **1977**, *99*, 5953. (f) Espenson, J. H.; Melton, J. D. *Inorg. Chem.* **1983**, *22*, 2779. (g) Smith J. R. L.; Balasubramanian, P. N.; Bruce, T. C. *J. Am. Chem. Soc.* **1988**, *110*, 7411. (h) Bruce, T. C. *Acc. Chem. Res.* **1991**, *24*, 243. (i) Ma, R.; Bakac, A.; Espenson, J. H. *Inorg. Chem.* **1992**, *31*, 1925. (j) Yao, Q.; Bakac, A.; Espenson, J. H. *Inorg. Chem.* **1993**, *32*, 1488.
- (3) (a) Bayston, J. H.; Beale, R. N.; King, N. K.; Winfield, M. E. *Aust. J. Chem.* **1963**, *16*, 954. (b) Roberts, H. L.; Symes, W. R. *J. Chem. Soc. A* **1968**, 1450. (c) Michelin, R. A.; Ros, R.; Strukul, G. *Inorg. Chim. Acta* **1979**, *37*, L491. (d) Wong, C. -L.; Endicott, J. F. *Inorg. Chem.* **1981**, *20*, 2333. (e) Geiger, T.; Anson, F. C. *J. Am. Chem. Soc.* **1981**, *103*, 7489. (f) Strukul, G.; Michelin, R. A. *J. Am. Chem. Soc.* **1985**, *107*, 7971. (g) Suzuki, H.; Matsuura, S.; Moro-Oka, Y.; Ikawa, T. *J. Organomet. Chem.* **1985**, *286*, 247. (h) Karlin, K. D.; Ghosh, P.; Cruse, R. W.; Farooq, A.; Gultneh, Y.; Jacobson, R. R.; Blackburn, N. J.; Strange, R. W.; Zubieta, J. *J. Am. Chem. Soc.* **1988**, *110*, 6769. (i) Wu, Y.-D.; Houk, K. N.; Valentine, J. S.; Nam, W. *Inorg. Chem.* **1992**, *31*, 718. (j) Mahroof-Tahir, M.; Murthy, N. N.; Karlin, K. D.; Blackburn, N. J.; Shaikh, S. N.; Zubieta, J. *Inorg. Chem.* **1992**, *31*, 3001. (k) Guajardo, R. J.; Hudson, S. E.; Brown, S. J.; Mascharak, P. K. *J. Am. Chem. Soc.* **1993**, *115*, 7971. (l) Wang, W.-D.; Bakac, A.; Espenson, J. H. *Inorg. Chem.* **1993**, *32*, 2205. (m) Wang, W.-D.; Bakac, A.; Espenson, J. H. *Inorg. Chem.* **1993**, *32*, 5034. (n) Guajardo, R. J.; Tan, J. D.; Mascharak, P. K. *Inorg. Chem.* **1994**, *33*, 2838. (o) Carmona, D.; Lamata, M. P.; Ferrer, J.; Modrego, J.; Perales, M.; Lahoz, F. J.; Atencio, R.; Oro, L. A. *J. Chem. Soc., Chem. Commun.* **1994**, 575.

(4) Walling, C. *Acc. Chem. Res.* **1975**, *8*, 125.

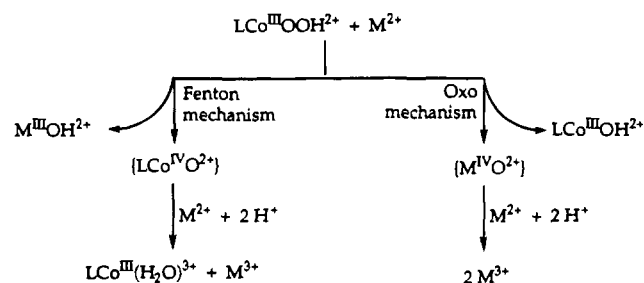
(5) (a) Groves, J. T.; Puy, M. V. D. *J. Am. Chem. Soc.* **1976**, *98*, 5290. (b) Sugimoto, H.; Sawyer, D. T. *J. Am. Chem. Soc.* **1984**, *106*, 4283.

(6) Traylor, T. G.; Xu, F. *J. Am. Chem. Soc.* **1987**, *109*, 6201.

(7) Scott, S. L.; Bakac, A.; Espenson, J. H. *J. Am. Chem. Soc.* **1992**, *114*, 4205.

(8) Kumar, K.; Endicott, J. F. *Inorg. Chem.* **1984**, *23*, 2447.

Scheme 1

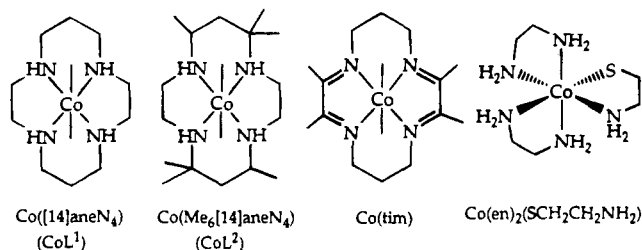


Hydrogen peroxide and organic hydroperoxides can be oxidized by a number of reagents, all of which are powerful electron acceptors. Typical reagents are Ce(IV),⁹ $M(\text{bpy})_3^{3+}$ ($M = \text{Os, Fe, Ru, and Ni}$),¹⁰ Mn^{3+} ,¹¹ Ag^{3+} ,¹² and Co^{3+} .¹³ Oxidation of $(\text{H}_2\text{O})_5\text{CrOOH}^{2+}$ by Ce(IV) and CrO^{2+} is also known.^{31,m}

In this paper, we report kinetic and mechanistic studies on the reductions and oxidations of LCoOOH^{2+} by transition metal complexes. The mechanisms for both types of reactions will be described in terms of the kinetic and other data, and their implications will be discussed.

Experimental Section

Reagents. 1,4,8,11-Tetraazacyclotetradecane ($= [14]\text{janeN}_4 = \text{L}^1$, Lancaster), $\text{Ru}(\text{NH}_3)_6\text{Cl}_3$ (Johnson Matthey) and $(\text{NH}_4)_2\text{IrCl}_6$ (Aldrich) were used as received. The solvent used throughout was water, distilled and deionized by passing through a Millipore-Q purification system. The preparation and analysis of aqueous solutions of $\text{Co}(\text{tim})^{2+}$, $\text{Fe}_{\text{aq}}^{2+}$, $\text{Fe}_{\text{aq}}^{3+}$, $(\text{en})_2\text{Co}(\text{SCH}_2\text{CH}_2\text{NH}_2)^{2+}$, and $\text{Ru}(\text{NH}_3)_6^{2+}$ have been described previously.^{31,m} Literature procedures were used to prepare $\text{Ru}(\text{bipy})_3(\text{ClO}_4)_3$,¹⁴ $\text{Fe}(\text{phen})_3(\text{ClO}_4)_3$,¹⁵ and $\text{L}^2\text{Co}(\text{H}_2\text{O})_2(\text{CF}_3\text{SO}_3)_2$.¹⁶ The structural formulas of the cobalt complexes (charges omitted) are as follows:



Solutions of $\text{L}^1\text{CoOOH}^{2+}$ were prepared by a slight modification of the literature procedure.⁸ The cobalt(II) complex $\text{L}^1\text{Co}(\text{H}_2\text{O})_2^{2+}$ was first prepared in H_2O and then the solution was acidified to a desired pH by the addition of trifluoromethanesulfonic acid. Oxygen was then passed through a solution containing equal concentrations of $\text{Ru}(\text{NH}_3)_6^{2+}$ and $\text{L}^1\text{Co}(\text{H}_2\text{O})_2^{2+}$ for 20 min at 0°C . The role of $\text{Ru}(\text{NH}_3)_6^{2+}$ is to reduce the initial product, $(\text{H}_2\text{O})\text{L}^1\text{CoO}_2^{2+}$, to $(\text{H}_2\text{O})\text{L}^1\text{CoOOH}^{2+}$. The UV-vis spectrum of the resulting solution is identical to that reported for $\text{L}^1\text{CoOOH}^{2+}$.^{3e} In other cases, where the $\text{Ru}(\text{NH}_3)_6^{3+}$ product would interfere with subsequent kinetic or stoichiometric measurements, the $\text{L}^1\text{Co}(\text{H}_2\text{O})_2^{2+}$ solution was instead prepared in perchloric acid so that the $\text{Ru}(\text{NH}_3)_6^{3+}$ ions were precipitated as $[\text{Ru}(\text{NH}_3)_6](\text{ClO}_4)_3$ and removed by filtration. Identical kinetics were observed for reactions of Fe^{2+} with $\text{L}^1\text{CoOOH}^{2+}$ from both sources. This is also true for the oxidation of $\text{L}^1\text{CoOOH}^{2+}$ by Fe^{3+} , which takes place with a rate constant $2.74 \pm 0.07 \text{ L mol}^{-1} \text{ s}^{-1}$ in $0.10 \text{ M CF}_3\text{SO}_3\text{H}$ compared with $2.80 \pm 0.10 \text{ L mol}^{-1} \text{ s}^{-1}$ in 0.10 M HClO_4 .

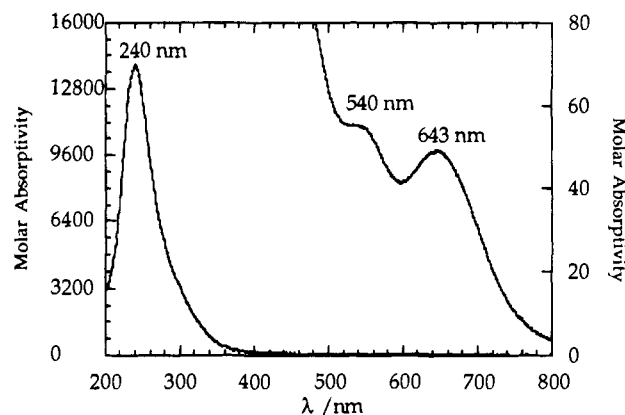


Figure 1. UV-vis spectrum of $\text{L}^2\text{CoOOH}^{2+}$ ($\text{L}^2 = \text{Me}_6[14]\text{janeN}_4$) in $0.10 \text{ M CF}_3\text{SO}_3\text{H}$.

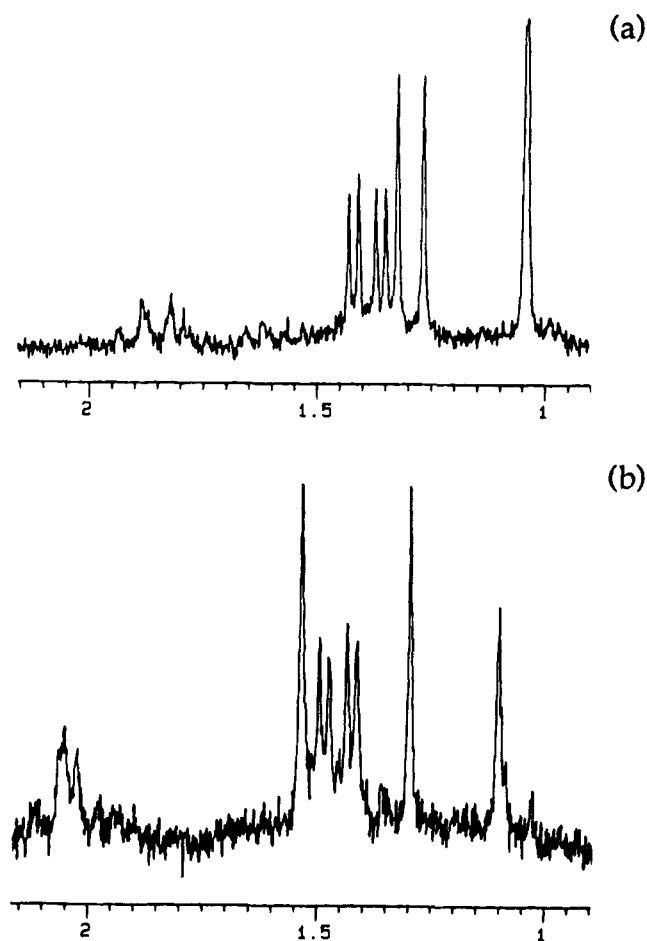


Figure 2. Proton NMR spectra: (a) $\text{L}^2\text{CoOOH}^{2+}$ ($\text{L}^2 = \text{Me}_6[14]\text{janeN}_4$) in D_2O ; (b) ligand-modified product of the $\text{L}^2\text{CoOOH}^{2+}/\text{Fe}^{2+}$ reaction in D_2O .

The above procedures were also used to prepare the analogous complex $\text{L}^2\text{CoOOH}^{2+}$. Both $\text{L}^1\text{CoOOH}^{2+}$ and $\text{L}^2\text{CoOOH}^{2+}$ solutions can be further purified by cation-exchange using Sephadex C-25 resin. To avoid decomposition of LCoOOH^{2+} on the column, the resin was pretreated with $1.0 \text{ M H}_2\text{O}_2$ and the separation process was conducted at 0°C . The kinetics of the redox reactions of Fe^{2+} or Fe^{3+} with chromatographically purified $\text{L}^1\text{CoOOH}^{2+}$ were the same as those using unpurified $\text{L}^1\text{CoOOH}^{2+}$.

Compared with the green solution of $\text{L}^1\text{CoOOH}^{2+}$, the solution of $\text{L}^2\text{CoOOH}^{2+}$ is greenish-yellow. The UV-vis spectra of the two hydroperoxides are similar; that of $\text{L}^2\text{CoOOH}^{2+}$ is shown in Figure 1. The proton NMR spectrum of the isolated $[\text{L}^2\text{Co}(\text{H}_2\text{O})(\text{OOH})](\text{ClO}_4)_2$ in D_2O is shown in Figure 2a. The two doublets at 1.36 and 1.42 ppm with a coupling constant of 6.3 Hz are from the CH-bound methyl groups of the macrocyclic ligand. The six inequivalent methyl groups

(9) Samuni, A.; Czapski, G. *J. Chem. Soc., Dalton Trans.* **1973**, 487.

(10) Macartney, D. H. *Can. J. Chem.* **1986**, *64*, 1936.

(11) Wells, C. F.; Fox, D. *J. Chem. Soc., Dalton Trans.* **1968**, 665.

(12) Borish, E. T.; Kirschenbaum, L. J. *J. Chem. Soc., Dalton Trans.* **1983**, 749.

(13) Davies, G.; Watkins, K. O. *J. Phys. Chem.* **1970**, *74*, 3388.

(14) Braddock, J. N.; Meyer, T. J. *J. Am. Chem. Soc.* **1973**, *95*, 3158.

(15) Ford-Smith, M. H.; Sutin, N. *J. Am. Chem. Soc.* **1961**, *83*, 1830.

(16) Bakac, A.; Espenson, J. H. *J. Am. Chem. Soc.* **1990**, *112*, 2273.

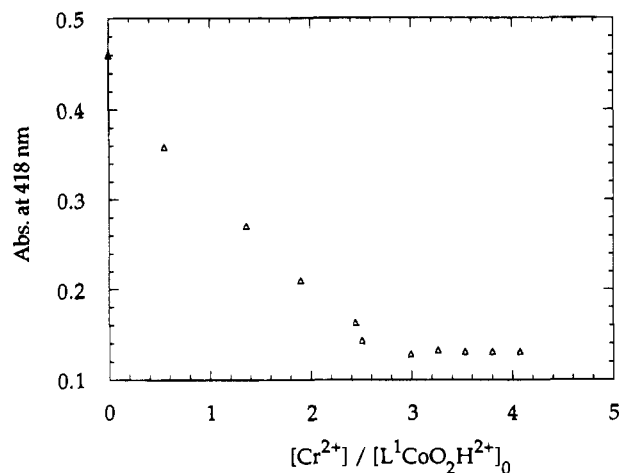


Figure 3. Absorbance at 418 nm (measured at 100-second intervals in a cell with 1-cm optical path) decreasing after each incremental addition of a solution of 36 mM Cr²⁺ to a solution of L¹CoOOH²⁺ (L¹ = [14]aneN₄), initially 2.0 mM, at 0.10 M H₃O⁺ under anaerobic conditions.

result in five signals in the range 1.0 to 1.5 ppm, in the ratio of 2:1:1:1:1. For compounds with two identical axial ligands, such as *trans*-[L²Co(H₂O)₂](ClO₄)₃ and *trans*-[L²CoCl₂](ClO₄)₂, only three types of methyl groups can be observed in the NMR spectra. On the basis of the NMR data, the complex [L²Co(H₂O)(OOH)](ClO₄)₂ is proposed to retain a *trans* structure with H₂O and OOH as the axial ligands.

Ion-exchange chromatography was used to confirm that the LCoOOH²⁺ complexes are indeed dications. For example, L¹CoOOH²⁺ is eluted with 0.4 M LiSO₃CF₃–0.1 M HSO₃CF₃ from the column of Sephadex C-25 after L¹CoCl₂⁺ and L¹Co(H₂O)Cl²⁺. Furthermore, the elution properties of L²CoOOH²⁺ are comparable to those of (Me₆[14]dieneN₄)Co(H₂O)Cl²⁺ and L¹Ni²⁺.

Kinetics. Kinetic measurements for reactions with half-lives > 10 s were carried out by use of a Shimadzu UV-2101PC and UV-3101PC spectrophotometers. A DX-17MV stopped-flow spectrophotometer from Applied Photophysics Ltd. was used for reactions with half-lives < 10 s. Most of the kinetic studies were conducted at 25.0 ± 0.2 °C and 0.10 M ionic strength, maintained with perchloric acid or trifluoromethanesulfonic acid. The activation parameters were evaluated over the temperature range 5–40 °C, controlled to within ±0.2 °C. When the acidity was varied, the ionic strength was maintained with LiClO₄ or LiSO₃CF₃. Unless stated otherwise, kinetic experiments were conducted under pseudo-first-order conditions with LCoOOH²⁺ as the limiting reagent. The absorbance (*D*)–time data were fitted to the equation $D_t = D_\infty + (D_0 - D_\infty) \exp(-k_p t)$. The second-order rate constants were obtained as the least-squares slopes of k_p versus the concentration of the excess reagent at the midpoint of the run. The formation of O₂ was detected with a portable Dissolved Oxygen Meter-16046 from Hach Chemical Co.

For experiments in the absence of Cl⁻, solutions of L¹CoOOH²⁺ were prepared by the reduction of an O₂-saturated solution of L¹Co(H₂O)₂³⁺ with [Ru(NH₃)₆](SO₃CF₃)₂. For this purpose, [Ru(NH₃)₆](SO₃CF₃)₃ was prepared from [Ru(NH₃)₆]Cl₃ and AgSO₃CF₃, and reduced on Zn/Hg. Identical kinetics were observed for the redox reactions carried out with and without Cl⁻.

Crystallographic Analysis of [L¹CoCl₂](ClO₄)₂. A crystal was attached to the tip of a glass fiber and mounted on the P4RA diffractometer for data collection at -50 ± 1 °C. The cell constants were determined from reflections found from a rotation photograph. A total of 2402 reflections were collected, and refinement calculations were performed on a Digital Equipment MicroVAX 3100 computer using the SHELXTL-Plus program.

Results

Reduction of L¹CoOOH²⁺. Cr²⁺. A spectrophotometric titration at 418 nm, Figure 3, showed that 3 mol of Cr²⁺ was consumed per mole of L¹CoOOH²⁺. The consumption of 2 mol of Cr²⁺ is required by both the Fenton and oxo mechanisms in one stage, (eq 1, M = Cr²⁺), but in itself it does not advocate

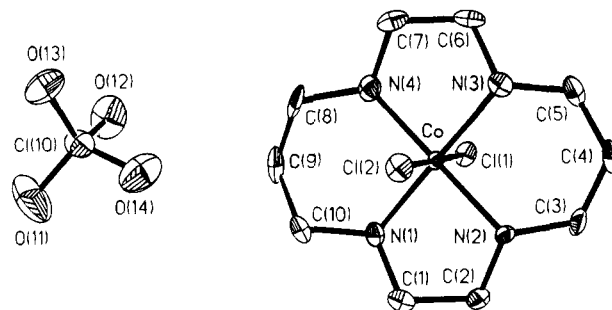
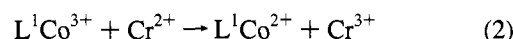
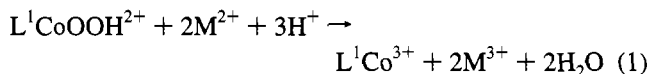


Figure 4. ORTEP view of [L¹CoCl₂](ClO₄)₂ provided at 50% probability. L¹ = 14[ane]N₄.

either, and the reduction of Co(III) accounts for the third mole of Cr²⁺, eq 2.



The kinetic data were collected at 280 nm. Excellent fits of the absorbance time profiles to a single exponential when Cr²⁺ was present in large excess suggest that reaction 2 is indeed too rapid to be evaluated as part of the reduction of L¹CoOOH²⁺. The value of the rate constant so obtained for reaction 1, eq 3, is (8.4 ± 0.2) × 10³ L mol⁻¹ s⁻¹.



Reaction 1 is a two-step process involving the formation of an intermediate and its rapid reaction with the second mole of Cr²⁺. The identities of the two steps depend on the mechanism being followed, as shown in Scheme 1.

Reaction 2 could be studied independently, starting directly with L¹Co(H₂O)₂³⁺. In the absence of Cl⁻, reaction 2 has $k = 3.8 \times 10^4$ L mol⁻¹ s⁻¹. Many experiments contained chloride ion from Ru(NH₃)₆Cl₃, used in the preparation of L¹CoOOH²⁺. Reductions of cobalt complexes by Cr²⁺ are in general greatly enhanced by bridging ligands like Cl⁻.^{17,18} The cobalt products of reaction 1, abbreviated simply as L¹Co³⁺, are actually a mixture of the chloro and aqua complexes, L¹CoCl₂⁺, L¹Co(H₂O)Cl²⁺ and L¹Co(H₂O)₂³⁺.

Fe²⁺. The UV–vis spectra of spent reaction solutions showed maxima at 240 nm (typical of Fe³⁺) and 580 nm (L¹-Co(III) products). The latter peak slowly shifted to 604 nm after a stable absorbance reading had been reached in the UV. Green crystals suitable for X-ray diffraction were obtained in 36% isolated yield from the reaction of 3.0 mM L¹CoOOH²⁺ with 0.033 mM Fe²⁺. The structure of the green crystal clearly identifies it as *trans*-L¹CoCl₂⁺, as shown in the ORTEP view in Figure 4.

The stoichiometry of the reaction is not simple, but it can be understood in terms of the competing steps. The stoichiometry was determined by titrating the reaction products with Cr²⁺, Figure 5, when a limiting amount of L¹CoOOH²⁺ was used. The endpoint was taken as the point at which the absorbance no longer changed and the isosbestic point was lost. The endpoint required 0.94 and 1.7 equiv of Cr²⁺, compared with [L¹CoOOH²⁺]₀, at ratios of [Fe²⁺]₀/[L¹CoO₂H²⁺]₀ of 1.3 and 6.4, respectively. However, as shown in Figure 5, 3 equiv of Cr²⁺ was needed when a large excess of Fe²⁺ was used, indicating that the reaction of L¹CoOOH²⁺ with Fe²⁺ produced 1 mol of L¹Co³⁺ and 2 mol of Fe³⁺. Direct analyses of [Fe³⁺],

(17) Liteplo, M. A.; Endicott, J. F. *Inorg. Chem.* **1971**, *10*, 1420.

(18) Rillema, D. P.; Endicott, J. F. *J. Am. Chem. Soc.* **1972**, *94*, 394.

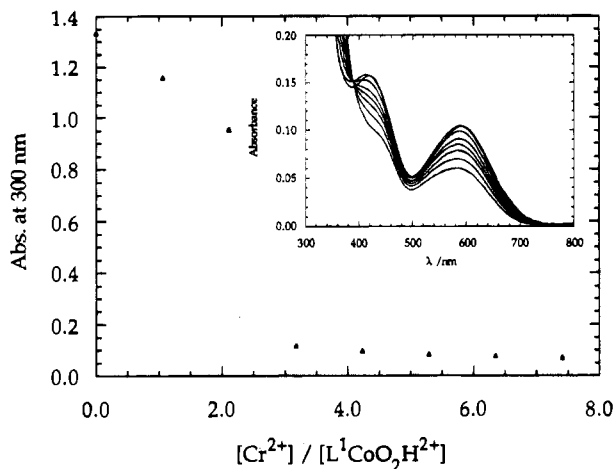


Figure 5. Spectrophotometric titration of a solution initially containing 0.56 mM L^1CoOOH^{2+} ($L^1 = [14]aneN_4$) and 40 mM Fe^{2+} with 36 mM Cr^{2+} . The reaction of L^1CoOOH^{2+} with Fe^{2+} was allowed to proceed to a stable absorbance reading before addition of Cr^{2+} . Inset: titration of a solution initially containing 2.0 mM L^1CoOOH^{2+} and 13.6 mM Fe^{2+} with 36 mM Cr^{2+} . The intermittent spectra were recorded at 100-s intervals.

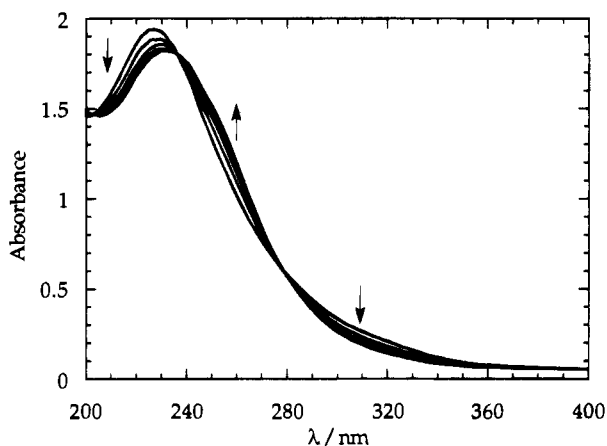


Figure 6. Repetitive-scan spectra of the reaction of L^1CoOOH^{2+} (0.12 mM, $L^1 = [14]aneN_4$) with VO^{2+} (0.42 mM) at 25 °C and 0.10 M H^+ . Scans were taken at intervals of 100 s.

identified and quantitated as $Fe^{III}\text{-}NCS^-$ complexes and calibrated with known concentrations, are in agreement with the stoichiometry of eq 1 ($M = Fe$). For example, the ratio $[Fe^{3+}]/[L^1CoOOH^{2+}]_0 = 1.8$ was calculated for the reaction of 0.050 mM L^1CoOOH^{2+} with 3.0 mM Fe^{2+} .

The conclusion is this: the Fe^{2+} reaction proceeds "normally" (by which we mean its stoichiometry corresponds to eq 1) when Fe^{2+} is used in large excess. With lesser amounts of Fe^{2+} , on the other hand, considerably more L^1CoOOH^{2+} is consumed (or considerably less Fe^{3+} is formed) than eq 1 specifies.

The kinetics of the reaction of L^1CoOOH^{2+} with Fe^{2+} were monitored at 320 nm. The reaction has a second-order rate constant $4.8 \pm 0.2 \text{ L mol}^{-1} \text{ s}^{-1}$ at $\mu = 0.10 \text{ M}$ and $9.7 \pm 0.5 \text{ L mol}^{-1} \text{ s}^{-1}$ at $\mu = 0.50 \text{ M}$.

VO^{2+} , V^{2+} , Ti^{3+} , and $Co(tim)^{2+}$. These reactions were studied mainly to evaluate the rate constant (the equivalent of k_1). Repetitive scan spectra of the L^1CoOOH^{2+}/VO^{2+} reaction, shown in Figure 6, indicated that this reaction could be easily followed spectrophotometrically. The kinetics were monitored at 320 nm. The second-order rate constants for VO^{2+} are 1.43 ± 0.05 and $2.7 \pm 0.1 \text{ L mol}^{-1} \text{ s}^{-1}$ at $\mu = 0.10$ and 0.50 M , respectively. The reduction of L^1CoOOH^{2+} by V^{2+} took place with a rate constant of $5.5 \pm 0.1 \text{ L mol}^{-1} \text{ s}^{-1}$, independent of $[H_3O^+]$ in the range 0.026–0.10 M at a constant ionic strength of 0.10 M. The second-order rate constant increased to $12.6 \pm$

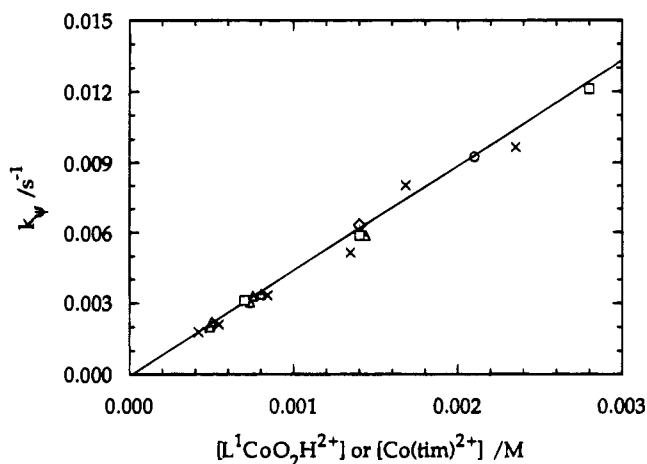


Figure 7. Plot of k_p against $[Co(tim)^{2+}]$ or $[L^1CoOOH^{2+}]$ ($L^1 = [14]aneN_4$). Conditions: 25 °C; $\mu = 0.10 \text{ M}$. $Co(tim)^{2+}$ in excess, $[H^+] = 0.010 \text{ M}$ (\square), 0.049 M (\circ), 0.064 M (\diamond), and 0.10 M (Δ). $L^1CoO_2H^{2+}$ in excess, $[H^+] = 0.10 \text{ M}$ (\times).

$0.2 \text{ M}^{-1} \text{ s}^{-1}$ at ionic strength of 0.50 M. The kinetic measurements were conducted at 260 nm. The reaction of L^1CoOOH^{2+} with Ti^{3+} , the slowest of the reduction reactions studied here, has a rate constant of $1.8 \pm 0.2 \text{ L mol}^{-1} \text{ s}^{-1}$ at 39.6 °C, with $[H^+] = 0.10 \text{ M}$ and $\mu = 0.5 \text{ M}$.

The stoichiometry of the $Co(tim)^{2+}$ reaction was determined kinetically. As shown in Figure 7, the pseudo-first-order rate constants are linearly proportional to the concentration of excess reagent, $[Co(tim)^{2+}]$ or $[L^1CoOOH^{2+}]$, and all the points fall on the same line, establishing the 1:1 reaction stoichiometry. (Were it 1:2, the slopes would have differed by a factor of 2, since the expressions for the reaction rate when the two concentrations are alternately in excess would have differed by this factor.) Furthermore, the absorbance changes at 453 nm that occur upon addition of limiting amounts of L^1CoOOH^{2+} to $Co(tim)^{2+}$ are in agreement with $\Delta[Co(tim)^{2+}] = [L^1CoOOH^{2+}]_0$. The $L^1CoOOH^{2+}/Co(tim)^{2+}$ reaction takes place with a second-order rate constant of $4.5 \pm 0.1 \text{ L mol}^{-1} \text{ s}^{-1}$. The kinetics of this reaction are independent of $[H_3O^+]$ in the range 0.010–0.10 M, as indicated in Figure 7.

Reduction of L^1CoOOH^{2+} in the Presence of $ArOH$. The compound 2-methyl-2-(3,5-di-*tert*-butyl-4-hydroxyphenyl)propyl]ammonium chloride, $ArOH$, is a water-soluble version of tri-*tert*-butylphenol that has been used as a trap for strongly oxidizing intermediates.^{31,3m,19,20} It can be oxidized to the persistent oxyl radical ArO^{\bullet} , which has a distinct visible spectrum. When the reaction of 0.15 mM L^1CoOOH^{2+} with 0.70 mM Fe^{2+} was carried out in the presence of 5.8 mM $ArOH$, ArO^{\bullet} could not be detected. Moreover, there was no ArO^{\bullet} generated from the $L^1CoOOH^{2+}/ArOH/VO^{2+}$ reactions.

Variations of $[H_3O^+]$, Temperature, and Ionic Strength. The rate constant for the Fe^{2+} reaction was studied at variable $[H_3O^+]$, at a constant ionic strength of 0.10 M, maintained with lithium triflate. The second-order rate constants are 4.79 ± 0.08 , 4.91 ± 0.08 , and $4.86 \pm 0.04 \text{ L mol}^{-1} \text{ s}^{-1}$, at $[H_3O^+] = 0.010$, 0.050, and 0.10 M. Similarly, the rate constants for the reactions of V^{2+} and $Co(tim)^{2+}$ with L^1CoOOH^{2+} were invariant over a range of $[H_3O^+]$ of 0.010–0.10 M.

Each of the rate constants, except that for Cr^{2+} , were determined as a function of temperature. Analysis according to transition state theory gave the values of ΔS^\ddagger and ΔH^\ddagger in Table 1.

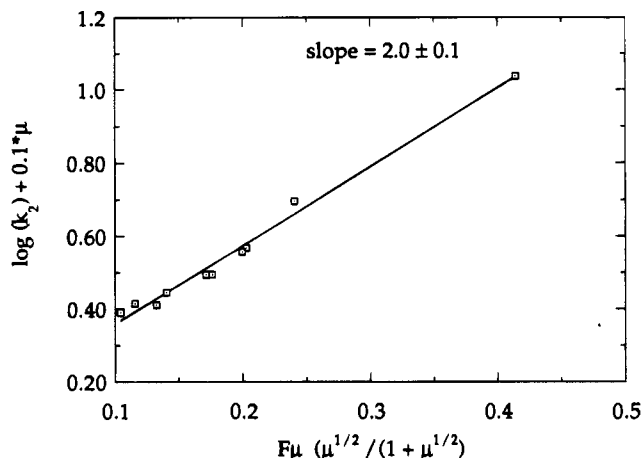
(19) Traylor, T. G.; Lee, W. A.; Stynes, D. V. *J. Am. Chem. Soc.* **1984**, *106*, 755.

(20) Al-Ajlouni, A.; Bakac, A.; Espenson, J. H. *Inorg. Chem.* **1993**, *32*, 5792.

Table 1. Rate Constants and Activation Parameters for the Reduction of L^1CoOOH^{2+} ^a

reductant	k_{298K}/L $mol^{-1} s^{-1}$	$\Delta H^\ddagger/kJ$ mol^{-1}	$\Delta S^\ddagger/J$ $mol^{-1} K^{-1}$
$Cr(H_2O)_6^{2+}$	$(8.4 \pm 0.2) \times 10^3$		
$Fe(H_2O)_6^{2+}$	4.86 ± 0.05	32.6 ± 0.9	-122 ± 5
$Co(tim)^{2+}$	4.5 ± 0.1	46.6 ± 2.6	-76.6 ± 8.9
$V(H_2O)_6^{2+}$	5.5 ± 0.1	23.1 ± 0.3	-153 ± 2
VO_2^{2+}	1.43 ± 0.05	47.6 ± 1.0	-82.1 ± 4.0
$(en)_2Co(SCH_2CH_2NH_2)^{2+}$	4.8 ± 0.2		

^a $[H_3O^+] = \mu = 0.10$ M, $L^1 = [14]aneN_4$.

**Figure 8.** Illustration of the ionic strength effect on the reaction between L^1CoOOH^{2+} ($L^1 = 14[ane]N_4$) and Fe^{2+} , plotted according to the Brønsted–Debye–Hückel equation.**Table 2.** Selected Bond Distances (Å) for $(L^1CoCl_2)ClO_4$ ($L^1 = [14]aneN_4$)

Co–Cl(1)	2.255(2)	Co–Cl(2)	2.257(2)
Co–N(1)	1.969(5)	Co–N(2)	1.962(4)
Co–N(3)	1.969(4)	Co–N(4)	1.961(5)

Table 3. Selected Bond Angles (deg) for $(L^1CoCl_2)ClO_4$ ($L^1 = [14]aneN_4$)

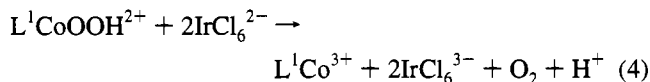
Cl(1)–Co–Cl(2)	179.2(1)	Cl(1)–Co–N(1)	88.1(1)
N(1)–Co–N(3)	179.3(2)	N(1)–Co–N(2)	85.7(2)
N(2)–Co–N(4)	179.1(2)	Co–N(1)–C(1)	108.2(3)

The rate constants for the Fe^{2+} and V^{2+} reactions were evaluated as a function of ionic strength. For Fe^{2+} , the ionic strength was varied in the range 0.014–0.50 M. As expected for a bimolecular reaction between cations, the rate constant increased with an increase in ionic strength. This can be displayed as in Figure 8, which presents the data in the form required by the Brønsted–Debye–Hückel equation. An extended form was used, to accommodate the results at the higher ionic strengths.²¹ The figure shows a plot of $\log k + 0.1 \mu$ vs $\mu^{1/2}/(1 + \mu^{1/2})$. The slopes of the plots are 2.1 for Fe^{2+} and 2.2 for V^{2+} .

X-ray Crystal Structure of $(L^1CoCl_2)ClO_4$. The structure of this complex, shown in Figure 4, was determined to establish unequivocally that it is a product of the reaction between L^1CoOOH^{2+} and Fe^{2+} . The cobalt atom is coplanar with the four nitrogen atoms. The bond distances and angles in the cobalt-macrocyclic ligand core are essentially the same as those found in other cobalt(III)– L^1 complexes.²² Selected bond distances and angles are given in Tables 2 and 3.

Oxidation of L^1CoOOH^{2+} . $IrCl_6^{2-}$. The ions $Ru(NH_3)_6^{3+}$ and $IrCl_6^{3-}$ form a suspension, which interferes with the

spectrophotometric studies. Therefore the L^1CoOOH^{2+} used in this reaction was prepared in $HClO_4$, and $[Ru(NH_3)_6](ClO_4)_3$ was removed by filtration, as described in the Experimental Section. The absorbance change at 488 nm is mainly due to $IrCl_6^{2-}$ ($\epsilon_{488} = 4075$ M⁻¹ cm⁻¹).²³ These changes were used to calculate the stoichiometry of eq 4.



The kinetics of the oxidation of L^1CoOOH^{2+} by $IrCl_6^{2-}$ are acid-dependent in the range 0.025–1.0 M H_3O^+ at $\mu = 1.0$ M. The second-order rate constant is linearly proportional to $1/[H_3O^+]$, the relationship being described by the equation k/L mol⁻¹ s⁻¹ = $(190 \pm 9) + (9.2 \pm 0.5)/[H_3O^+]$ at 25.0 °C.

Ru(bipy)₃³⁺. Because of the low solubility of $Ru(bipy)_3^{3+}$ in perchlorate media, the oxidation of $L^1CoO_2H^{2+}$ was studied in HSO_3CF_3 and monitored at 453 nm. Under pseudo-first-order conditions with L^1CoOOH^{2+} as the limiting reagent, the kinetic data yielded a second-order rate constant of 2.2×10^3 L mol⁻¹ s⁻¹. With $[L^1CoOOH^{2+}]$ in 10-fold excess over $[Ru(bipy)_3^{3+}]$, the second-order rate constant, calculated as $k_p/[L^1CoOOH^{2+}]$, is 4.2×10^3 L mol⁻¹ s⁻¹. Thus the reaction of L^1CoOOH^{2+} with $Ru(bipy)_3^{3+}$ follows the 1:2 stoichiometry analogous to that shown in eq 4. The acid dependence was evaluated over the range 0.10–1.0 M H_3O^+ at 1.0 M ionic strength. A plot of the second-order rate constants against $1/[H_3O^+]$ is linear, as described by the equation k/L mol⁻¹ s⁻¹ = $(1510 \pm 570) + (793 \pm 94)/[H_3O^+]$.

Fe(phen)₃³⁺. The reaction with L^1CoOOH^{2+} in CF_3SO_3H was followed spectrophotometrically at 510 nm. The kinetic data established the 1:2 stoichiometry analogous to that in eq 4. The second-order rate constant is 191 L mol⁻¹ s⁻¹ at $[H_3O^+] = \mu = 1.0$ M. A study of the kinetic dependence on $[H_3O^+]$ was not carried out owing to the instability of $Fe(phen)_3^{3+}$ at low acidity.

Fe³⁺ and VO₂⁺. Oxygen, L^1Co^{3+} , and Fe^{2+} are the products of the oxidation of L^1CoOOH^{2+} by Fe^{3+} . When 4.3 mM Fe^{3+} was allowed to react with 1.0 mM L^1CoOOH^{2+} at 0.10 M H_3O^+ , 0.19 mM O_2 (19% yield) was detected by an oxygen electrode. The yield is less than quantitative because the Fe^{2+} product consumes significant amounts of L^1CoOOH^{2+} . Also, some O_2 is lost from the solution on the time scale of these experiments.

The cobalt(III) species were identified spectroscopically. The presence of Fe^{2+} was indicated by the formation of $Fe(phen)_3^{2+}$ after an aliquot of the reaction solution was added to a phenanthroline solution.

At $\mu = [H_3O^+] = 0.10$ M, the second-order rate constant is 2.8 ± 0.1 L mol⁻¹ s⁻¹, as determined spectrophotometrically. Kinetic studies were also performed by monitoring the formation of O_2 with the oxygen electrode. These data are consistent with the spectrophotometric results. As observed for the other oxidation reactions, the reaction of L^1CoOOH^{2+} with Fe^{3+} is accelerated at low $[H_3O^+]$. The mechanism will be discussed later.

The reaction of L^1CoOOH^{2+} with VO_2^{2+} was monitored at 320 nm. Unlike all the other oxidation reactions studied here, the second-order rate constant increases with increasing acidity. This is as expected for the conversion of VO_2^{2+} to VO^{2+} . For example, a second-order rate constant of 254 ± 3 L mol⁻¹ s⁻¹ was obtained at $[H_3O^+] = \mu = 1.0$ M, compared with 21 ± 1 L mol⁻¹ s⁻¹ at $\mu = 1.0$ M and $[H_3O^+] = 0.10$ M.

The kinetic data for the oxidation reactions, and the self-exchange rate constants and reduction potentials of the oxidants are summarized in Table 4.

(21) Wilkins, R. G. *Kinetics and Mechanisms of Reactions of Transition Metal Complexes*, 2nd ed.; VCH: New York, 1991; p 112.

(22) Bakac, A.; Espenson, J. H. *Inorg. Chem.* **1987**, *26*, 4353 and references therein.

(23) Poulson, I. A.; Garner, C. S. *J. Am. Chem. Soc.* **1962**, *84*, 2032.

Table 4. Rate Constants for the Oxidation of L^1CoOOH^{2+} ($L^1 = [14]janeN_4$) by Transition Metal Complexes and Related Data at 25.0 °C and 1.0 M H_3O^+

	$Fe(H_2O)_6^{3+}$	VO_2^+	$IrCl_6^{2-}$	$Fe(phen)_3^{3+}$	$Ru(bipy)_3^{3+}$
$k/L \text{ mol}^{-1} \text{ s}^{-1}$	0.44 ± 0.04	254 ± 3	195 ± 9	191 ± 9	2150 ± 90
$E_{1/2}/V^a$	0.77	1.01	0.86	1.01^b	1.26^c
$k_{ex}/L \text{ mol}^{-1} \text{ s}^{-1}$	4.0^d		$2 \times 10^3^e$	$1 \times 10^7^b$	$1 \times 10^7^c$

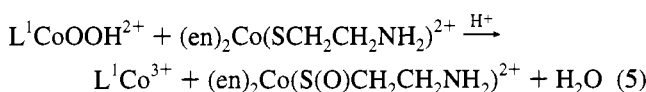
^a Shriver, D. F.; Atkins, P. W.; Langford, C. H. *Inorganic Chemistry*; W. H. Freeman: New York, 1990; pp 651–657. ^b Monsted, O.; Nord, G. *Adv. Inorg. Chem.* **1991**, *37*, 381. Larsen, D. W.; Wahl, A. C. *J. Am. Chem. Phys.* **1965**, *43*, 3765. ^c Braddock, J. N.; Meyer, T. J. *J. Am. Chem. Soc.* **1973**, *95*, 3158. ^d Silverman, J.; Dodson, R. W. *J. Phys. Chem.* **1952**, *56*, 846. ^e Hurwitz, P.; Kustin, K. *Trans. Faraday Soc.* **1966**, *62*, 427.

Table 5. Summary of Kinetic Data^a for the Redox Reactions of L^2CoOOH^{2+} and Related Reactions of L^1CoOOH^{2+}

reactants	$k_{298K}/L \text{ mol}^{-1} \text{ s}^{-1}$	
	L^2CoOOH^{2+}	L^1CoOOH^{2+}
Fe^{2+}	5.4 ± 0.2	4.86 ± 0.07
$Co(tim)^{2+}$	10.33 ± 0.07	4.5 ± 0.1
$IrCl_6^{2-}$	235 ± 10	390 ± 20

^a $[H_3O^+] = \mu = 0.10 \text{ M}$, $L^1 = [14]janeN_4$, $L^2 = Me_6[14]janeN_4$.

Oxygen Atom Transfer from L^1CoOOH^{2+} . The reaction between the cobalt-hydroperoxo complex and $(en)_2CoSCH_2CH_2NH_2^{2+}$ gives the sulfenato product shown in eq 5. This material was identified by its characteristic spectrum.^{3m} The reaction followed second-order kinetics, with $k = 5.0 \pm 0.2 \text{ L mol}^{-1} \text{ s}^{-1}$ at 25 °C and $[H_3O^+] = \mu = 0.10 \text{ M}$. The rate constant is directly proportional to the acid concentration, $k/L \text{ mol}^{-1} \text{ s}^{-1} = 0.20 + 52[H_3O^+]$ at $\mu = 0.10 \text{ M}$.



No reaction between L^1CoOOH^{2+} and PPh_3 was found to occur within 5 min at 25 °C and 0.10 M H_3O^+ in 1:1 CH_3CN/H_2O . Similarly, the water-soluble phosphine $Ph_2P(p-C_6H_4-SO_3Na)$ does not react with L^1CoOOH^{2+} .

Reactions of L^2CoOOH^{2+} . The kinetic data for the redox reactions of L^2CoOOH^{2+} with selected reagents are given in Table 5. Chromatographically purified L^2CoOOH^{2+} was used in all the kinetic experiments. As found in the L^1CoOOH^{2+} reactions, the reaction of L^2CoOOH^{2+} with $Co(tim)^{2+}$ proceeds with a 1:1 stoichiometry, and the reaction with $IrCl_6^{2-}$ with a 1:2 stoichiometry.

One of the cobalt products of the L^2CoOOH^{2+}/Fe^{2+} reaction is $L^2Co(H_2O)_2^{3+}$, identified by its NMR spectrum, which matched exactly that of a sample prepared by the oxidation of $L^2Co(H_2O)_2^{2+}$ with PbO_2 . The other product had a complicated NMR spectrum and was not identified. After this compound was separated from $L^2Co(H_2O)_2^{3+}$ by ion exchange chromatography, the NMR spectrum showed five signals of equal intensity in the region 1.0–2.0 ppm, Figure 2b.

Discussion

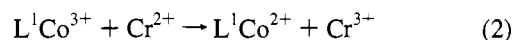
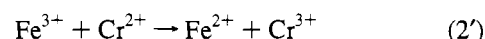
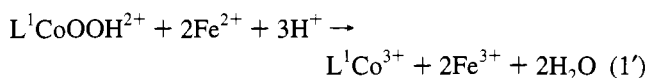
Reduction Reactions. Stoichiometry and Products. The 1:2 stoichiometry defined in eq 1 has been proved for the reaction of L^1CoOOH^{2+} with Cr^{2+} . Because the product L^1Co^{3+} is readily reduced to L^1Co^{2+} according to eq 2, another equivalent of Cr^{2+} is needed. As shown in Figure 3, a total of 3 equiv of Cr^{2+} was consumed in the reaction of L^1CoOOH^{2+} with Cr^{2+} .

The Cr^{3+} product was identified on the basis of the visible spectrum. The yield of $L^1Co(H_2O)_2^{2+}$ was calculated after the

contribution of 3 equiv of Cr^{3+} (compared with $[L^1CoOOH^{2+}]_0$) was subtracted from the spectrum of the final solution. The concentration of $L^1Co(H_2O)_2^{2+}$ based on the absorbance and the known molar absorptivity ($\epsilon_{470 \text{ nm}} = 33 \text{ M}^{-1} \text{ cm}^{-1}$)²⁴ is in agreement with the initial concentration of L^1CoOOH^{2+} .

In the L^1CoOOH^{2+}/Fe^{2+} reaction, the two stages in the titration curve, shown in Figure 5, can be correlated with eqs 1', 2' and 2 in Scheme 2.

Scheme 2



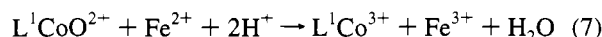
Equation 2' defines the stage in which 2 equiv of Cr^{2+} is consumed by the Fe^{3+} formed in eq 1'. Since the Fe^{3+} ion has a much weaker absorption at 300 nm than L^1Co^{3+} , the absorbance change is not dramatic. The sudden drop of absorbance upon adding the third equivalent of Cr^{2+} is caused by reaction of eq 2. This observation indicates that the rate constant for reaction 2' is much larger than that for reaction 2, which is in agreement with potentials of the Fe^{3+}/Fe^{2+} couple ($E_{1/2} = 0.77 \text{ V}$) and the L^1Co^{3+}/L^1Co^{2+} couple ($E_{1/2} = 0.42 \text{ V}$).^{3d,25}

For the reaction of L^1CoOOH^{2+} with a large excess of Fe^{2+} , the absorption maxima in the visible region slowly shifted from 580 nm to 604 nm after a stable absorbance in the UV region had been achieved. This slow absorbance change corresponds to the formation of neither $L^1Co(H_2O)_2^{3+}$ ($\lambda_{\text{max}} = 570 \text{ nm}$)^{3e} nor $L^1CoCl_2^+$ ($\lambda_{\text{max}} = 630 \text{ nm}$),²⁶ but it is likely to reflect equilibria among $L^1Co(H_2O)_2^{3+}$, $L^1Co(H_2O)Cl^{2+}$ and $L^1CoCl_2^+$. When chloride ions were removed by adding Ag^+ to the solution, the filtrate had the spectrum of $L^1Co(H_2O)_2^{3+}$.

Mechanism. Two mechanisms for the reduction of hydroperoxides by transition metal complexes have generally been accepted, Scheme 1. The Fenton mechanism is most likely involved in reactions carried out in aqueous solution and with aqua-metal reductants. The oxo transfer capability for reactions conducted in pure CH_3CN strongly support the two-electron process.^{5b}

The stoichiometry and products of the reaction of L^1CoOOH^{2+} with Cr^{2+} or with a large excess of Fe^{2+} agree with both mechanisms. The mechanism shown in Scheme 3, using the reaction with Fe^{2+} as an example, is preferred based on the stoichiometry of the reaction of L^1CoOOH^{2+} with a slight excess of Fe^{2+} , the trapping experiments, and the NMR spectra of the reaction products. Reaction 7 may involve $[LCoOFe]^{4+}$ as an intermediate, as shown in eqs 7a and 7b.

Scheme 3



The 1:2 stoichiometry of the L^1CoOOH^{2+}/Fe^{2+} reaction holds only when large excess of Fe^{2+} is used. After the reaction was

(24) Mok, C. Y.; Endicott, J. F. *J. Am. Chem. Soc.* **1978**, *100*, 123.

(25) Wong, C.-L.; Switzer, J. A.; Balakrishnan, K. P.; Endicott, J. F. *J. Am. Chem. Soc.* **1980**, *102*, 5511.

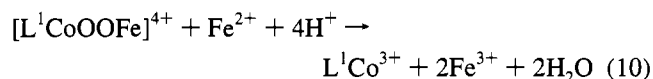
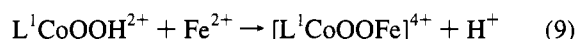
(26) Bosnich, B.; Poon, C. K.; Tobe, M. L. *Inorg. Chem.* **1965**, *4*, 1102.

completed, only 1.7 equiv of Cr^{2+} (compared with $[\text{L}^1\text{CoOOH}^{2+}]_0$), instead of 3 equiv, was needed to reach the titration end point when $[\text{Fe}^{2+}]_0/[\text{L}^1\text{CoOOH}^{2+}]_0 = 6.4/1$. It was found that the ratio of $[\text{Cr}^{2+}]_{\text{end}}/[\text{L}^1\text{CoOOH}^{2+}]_0$ increases with the initial ratio $[\text{Fe}^{2+}]_0/[\text{L}^1\text{CoOOH}^{2+}]_0$. This observation probably results from the competing reactions after the formation of an intermediate. The highly reactive intermediate $\text{L}^1\text{CoO}^{2+}$, generated in eq 6, can either oxidize Fe^{2+} to Fe^{3+} , which will lead to the 1:2 stoichiometry, or react intramolecularly with the macrocyclic ligand, eq 8, causing the stoichiometry to deviate from 1:2.



Both $\text{L}^1\text{CoO}^{2+}$ and FeO^{2+} are expected to oxidize ArOH to ArO^* , but no ArO^* was observed in the trapping experiments. Apparently, FeO^{2+} was not produced, and $\text{L}^1\text{CoO}^{2+}$, if formed, had undergone intramolecular ligand oxidation. When Cr^{2+} was used as reductant, then the bimolecular reaction of Cr^{2+} with $\text{L}^1\text{CoO}^{2+}$ is faster than intramolecular ligand oxidation owing to the strong reducing ability of Cr^{2+} . Therefore, the coordinated macrocyclic ligand is not oxidized during the titration of $\text{L}^1\text{CoOOH}^{2+}$ with Cr^{2+} .

Another mechanism that would fit the data equally well is shown in eqs 9 and 10, featuring a μ -peroxo intermediate that



is reduced rapidly by the second mole of Fe^{2+} . This mechanism is written in analogy with recent proposals for the reduction of H_2O_2 with transition metal complexes^{11-k} and in the present case draws support from the fact that a large number of μ -peroxo complexes exist and are known to react with reducing metals. The role of $[\text{LCoOFe}]^{4+}$ in the side reactions is expected to be analogous to that of $\text{L}^1\text{CoO}^{2+}$, and the final product distribution is determined by the competition between intramolecular and intermolecular processes.²⁷

Ionic Strength Effect and the Reactions with $\text{Co}(\text{tim})^{2+}$. The product $Z_A Z_B = 2$ ($A = \text{L}^1\text{CoOOH}^{2+}$; $B = \text{Fe}^{2+}$ or V^{2+}) was obtained from the plot of $\log k$ vs $\mu^{1/2}/(1+\mu^{1/2})$ according to the Bronsted-Debye-Hückel equation. This clearly contradicts the assignment of the reactants. The kinetics are independent of $[\text{H}_3\text{O}^+]$, which rules out reactions such as $\text{L}^1\text{CoOO}^+/\text{Fe}^{2+}$ or $\text{L}^1\text{CoOOH}^{2+}/\text{FeOH}^+$. The fact that both Fe^{2+} and V^{2+} are well-characterized species with a 2+ charge might lead one to conclude that the hydroperoxocobalt complex has a 1+ charge. However, the affinity of the complex for Sephadex C-25, and the lack of the chloride effect on kinetics argue against the involvement of *cis*- $\text{L}^1\text{Co}(\eta^2\text{-OO})^+$ or $\text{L}^1\text{CoCl}(\text{OOH})^+$. We cannot exclude the possibility of ion-pairing between one of the reactants and perchlorate ions.

The reaction of $\text{L}^1\text{CoOOH}^{2+}$ with $\text{Co}(\text{tim})^{2+}$ takes place with a 1:1 stoichiometry. The same observation was made in the analogous reactions of $\text{Co}(\text{tim})^{2+}$ with H_2O_2 and ROOH .^{1b} The utilization of both oxidizing equivalents of the peroxides clearly implicates the involvement of the macrocycle. The identity of the product(s) has not been established.

(27) When Fe^{2+} is present in a 3–4-fold excess over $\text{L}^1\text{CoOOH}^{2+}$, 36% of the total cobalt is converted to $\text{L}^1\text{CoCl}_2^+$. In the $\text{L}^2\text{CoOOH}^{2+}$ reaction, a comparable amount (33%) of the cobalt products is $\text{L}^2\text{Co}(\text{H}_2\text{O})_3^{3+}$. Only five methyl groups can be identified in the NMR spectrum of the remaining cobalt product. The two CH-bound methyl groups of the macrocycle are still present, and thus the ligand oxidation appears to have taken place at one of the $\text{C}(\text{CH}_3)_2$ groups.

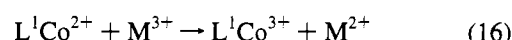
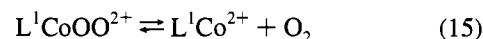
Site of Attack. All of the reactions of LCoOOH^{2+} ions with reductants have been written as taking place at the hydroperoxo site. We dismissed the possibility of direct involvement of the metal center in the hydroperoxo complexes based on the reactivity profile.

The reactivities of LCoOOH^{2+} complexes and H_2O_2 toward the reductants in Table 1 are similar and both series of reactions are independent of acidity. In contrast, the reduction at the cobalt would be expected to show similarities with the reduction of $(\text{H}_2\text{O})_2\text{CoL}^{3+}$ ions. Such reactions proceed either by an OH⁻-bridged, inner-sphere mechanism ($1/[\text{H}^+]$ -catalyzed), or by an outer sphere mechanism ($[\text{H}^+]$ -independent) with a different reactivity order than observed here. Specifically, $\text{Ru}(\text{NH}_3)_6^{2+}$ and $\text{V}(\text{H}_2\text{O})_6^{2+}$ are much more reactive outer-sphere reductants than $\text{Cr}(\text{H}_2\text{O})_6^{2+}$, yet the hydroperoxides LCoOOH^{2+} react rapidly with $\text{Cr}(\text{H}_2\text{O})_6^{2+}$, slowly with $\text{V}(\text{H}_2\text{O})_6^{2+}$, and not at all with $\text{Ru}(\text{NH}_3)_6^{2+}$.

Oxidation Reactions. In contrast to hydrogen peroxide, alkyl hydroperoxides, and $(\text{H}_2\text{O})_5\text{CrOOH}^{2+}$, the compound $\text{L}^1\text{CoOOH}^{2+}$ can be oxidized at a noticeable rate at $[\text{H}_3\text{O}^+] \geq 0.10$ M by mild oxidizing reagents, such as Fe^{3+} and IrCl_6^{2-} . The experimentally observed stoichiometry and the formation of O_2 are consistent with the reaction defined by eq 4. The reaction of $\text{L}^1\text{CoOOH}^{2+}$ with $[\text{Ru}(\text{NH}_3)_4(\text{phen})]^{3+}$ has been studied by Kumar and Endicott.⁸ An outer-sphere electron-transfer mechanism involving the acid-base equilibrium of the coordinated hydroperoxide was proposed. In this work, the oxidation of $\text{L}^1\text{CoOOH}^{2+}$ by reagents, some of which are well known outer-sphere oxidants, has been investigated.

Outer-Sphere Mechanism. On the basis of the acid-dependent kinetics, and the observed products and stoichiometry, the mechanism in Scheme 4 is proposed.

Scheme 4



The protolytic equilibria (eqs 11 and 13), the O_2 dissociation (eq 15),⁸ and the oxidation of L^1Co^{2+} (eq 16)²⁸ are fast compared with the reactions in eq 12. The reverse of reaction 15 can also be neglected owing to the fast subsequent reaction 16. Therefore, the rate law described by eq 17 is derived for Scheme 4. Equation 17 can be rewritten as eq 18 because $[\text{H}^+] \gg K_{11}$ ($\approx 10^{-8}$ M).⁸

$$k_{\psi} = \frac{k_{12}[\text{H}^+] + k_{14}K_{11}}{K_{11} + [\text{H}^+]}[\text{M}^{3+}] \quad (17)$$

$$k_{\psi} = \left(k_{12} + \frac{k_{14}K_{11}}{[\text{H}^+]} \right) [\text{M}^{3+}] \quad (18)$$

The acid-dependent kinetics for the oxidations with $\text{Ru}(\text{bipy})_3^{3+}$ and IrCl_6^{2-} fit eq 18 well. Computer simulation

(28) (a) Rillema, D. P.; Endicott, J. F. *J. Am. Chem. Soc.* **1972**, *94*, 8711. (b) Durham, B.; Endicott, J. F.; Wong, C.-L.; Rillema, D. P. *J. Am. Chem. Soc.* **1979**, *101*, 847.

(Kinsim)²⁹ according to Scheme 4 indicates that the kinetic traces can be fitted to a single exponential as long as $k_{16} \geq 10^3 \text{ L mol}^{-1} \text{ s}^{-1}$. For oxidants such as $\text{Ru}(\text{bipy})_3^{3+}$ and IrCl_6^{2-} , the corresponding rate constants are $k_{16} > 10^5 \text{ L mol}^{-1} \text{ s}^{-1}$.²⁸ Scheme 4 does not include the bimolecular reaction between L^1Co^{2+} and $\text{L}^1\text{CoOO}^{2+}$. The simulations show that this reaction is negligible under the experimental conditions because of the low steady state concentrations of both of these intermediates.

On the basis of the experimental data, we cannot completely rule out a direct reaction between $\text{L}^1\text{CoOO}^{2+}$ and M^{3+} , resulting in oxidative homolysis. Such a process has been observed for the related $(\text{H}_2\text{O})_5\text{CrOO}^{2+}$ ion,³⁰ and is expected to be more facile for $\text{L}^1\text{CoOO}^{2+}$. The net result would be identical with the sum of reactions 15 and 16.

If the oxidation reactions (eqs 12 and 14) occur by outer-sphere electron transfer, the corresponding rate constants on a relative scale should fit the Marcus square root relation, eq 19.³¹

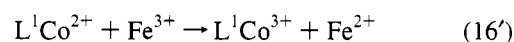
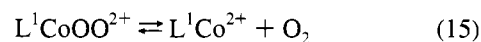
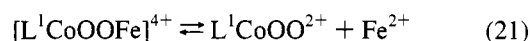
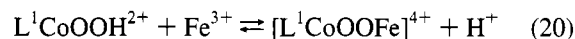
$$k_{ac} = k'_{bc} (10^{16.9(E-E')}) k_{aa}/k'_{bb})^{1/2} \quad (19)$$

Here k_{ac} and k'_{bc} are the rate constants for eq 12 or 14 for oxidants A and B, E and E' are their reduction potentials, and k_{aa} and k'_{bb} represent the self-exchange rate constants for oxidants A and B. Owing to the instability of the complex $\text{Fe}(\text{phen})_3^{3+}$, its rate constants k_{12} and k_{14} could not be obtained. If the self-exchange rate constants for $\text{L}^1\text{CoOOH}^{3+/2+}$ and $\text{L}^1\text{CoOO}^{2+/+}$ are similar, as assumed by Kumar and Endicott,⁸ the composite rate constants ($k_{12} + k_{14}K_{11}/[\text{H}_3\text{O}^+]$) for different oxidants can be directly compared. The relative values at $\mu = [\text{H}_3\text{O}^+] = 1.0 \text{ M}$ are 11 ($\text{Ru}(\text{bipy})_3^{3+}$):1 ($\text{Fe}(\text{phen})_3^{3+}$):1 (IrCl_6^{2-}). The calculated³² ones are in the order 16:1:0.10. The rough consistency with Marcus theory supports the outer-sphere electron-transfer mechanism for the oxidations of $\text{L}^1\text{CoOOH}^{2+}$ by these reagents.

Inner-Sphere Mechanism. With $\text{Fe}(\text{phen})_3^{3+}$ as reference, the rate constant of the $\text{L}^1\text{CoOOH}^{2+}/\text{Fe}^{3+}$ reaction, calculated from eq 19, is 10^3 times less than the experimental value. This result indicates that the oxidation of $\text{L}^1\text{CoOOH}^{2+}$ by Fe^{3+} may follow a different mechanism. An alternative is shown in Scheme 5. The acid-dependent kinetics observed for the Fe^{3+}

reaction is consistent with this scheme.³³ The same type of inner-sphere mechanism has been proposed for the oxidation of H_2O_2 by Fe^{3+} .³⁴

Scheme 5



The first intermediate in Scheme 5, $[\text{L}^1\text{CoOOFe}]^{4+}$, is identical to that produced in the reaction of $\text{L}^1\text{CoOO}^{2+}$ with Fe^{2+} ,^{3d} where it presumably decomposes to $\text{L}^1\text{CoOOH}^{2+}$ and Fe^{3+} . Both reactions 20 and 21 are written as equilibrium processes, which can be shifted by varying the concentrations of the reactants. Excess Fe^{3+} in the present work shifts the equilibrium toward $\text{L}^1\text{CoOO}^{2+}$ and Fe^{2+} .

Unlike that for other oxidation reactions, the second-order rate constant for the VO_2^+ reaction increases with increasing acidity. Neither eq 11 nor eq 20 can account for this observation. It is most likely that the kinetics of the VO_2^+ reaction is governed by the potential of the $\text{VO}_2^+/\text{VO}^{2+}$ couple, which is pH dependent as defined by $E = E^\circ - 0.118 \text{ pH}$.

Oxygen Atom Transfer Reaction. Oxygen transfer reactions involving hydrogen peroxide are well documented.³⁵ The rate law for the oxidation of nucleophiles is generally of the form³⁶

$$\text{rate} = k_0[\text{H}_2\text{O}_2][\text{Nuc}] + k_{\text{H}}[\text{H}_2\text{O}_2][\text{Nuc}][\text{H}^+] \quad (22)$$

The transformation of $(\text{en})_2\text{Co}(\text{SCH}_2\text{CH}_2\text{NH}_2)^{2+}$ to $(\text{en})_2\text{Co}(\text{S}(\text{O})\text{CH}_2\text{CH}_2\text{NH}_2)^{2+}$ mediated by $\text{L}^1\text{CoOOH}^{2+}$ follows the same rate law as the reaction with H_2O_2 ³⁷ and it probably takes place by nucleophilic attack at oxygen. Under the same conditions, $\text{L}^1\text{CoOOH}^{2+}$ ($k = 5.0 \text{ L mol}^{-1} \text{ s}^{-1}$ at 0.1 M H^+) reacts faster than H_2O_2 ($1.36 \text{ L mol}^{-1} \text{ s}^{-1}$),³⁷ but more slowly than $(\text{H}_2\text{O})_5\text{CrOOH}^{2+}$ ($20.5 \text{ L mol}^{-1} \text{ s}^{-1}$).^{3m} The positive charge on the metal center could enhance the electrophilicity of the peroxo ligand.

Acknowledgment. We are grateful to Dr. Victor G. Young, Jr., for the X-ray crystal structure determination. This work was supported by a grant from the National Science Foundation (CHE-9007283). Some of the experiments were conducted with the use of the facilities of the Ames Laboratory.

IC950080L

(29) Barshop, B. A.; Wrenn, R. A.; Frieden, C. *Anal. Biochem.* **1983**, *130*, 134.

(30) Bakac, A.; Espenson, J. H.; Janni, J. A. *J. Chem. Soc., Chem. Commun.* **1994**, 315.

(31) (a) Marcus, R. A. *Annu. Rev. Phys. Chem.* **1964**, *15*, 155. (b) Newton, T. W. *J. Chem. Educ.* **1968**, *45*, 571.

(32) Because the reactions involve reactants of different charges it is necessary to introduce corrections for work terms. The following equations were used to calculate the contribution of charges. (See: Zahir, K.; Espenson, J. H.; Bakac, A. *Inorg. Chem.* **1988**, *27*, 3144.) With respect to the W_{12} term, the $2-/2+$ reaction is favored over the $2+/2+$ reaction by a factor of 21.6 for $r = 8 \times 10^{-10} \text{ m}$, $\alpha = 1.76 \times 10^{-6} \text{ J mol}^{-1} \text{ m}$ and $\beta = 3.285 \times 10^9 \text{ m}^{-1} \text{ mol}^{-1/2} \text{ L}^{1/2} \text{ m}$.

$$k_{12} = (k_{11}k_{22}K_{12}f_{12})^{1/2}W_{12}$$

$$\ln f_{12} = \frac{[\ln K_{12} + (w_{12} - w_{21})/RT]^2}{4[\ln(k_{11}k_{22}/Z^2) + (w_{11} + w_{22})/RT]}$$

$$W_{12} = \exp[-(w_{12} + w_{21} - w_{11} - w_{22})/2RT]$$

$$w_{ij} = \frac{\alpha Z_i Z_j}{r(1 + \beta r \mu^{1/2})}$$

(33) The reverse of eq 21 can be neglected because the subsequent reactions are much faster than the reverse reaction. The following rate law can be derived: $[\text{Fe}^{3+}]/k_{\psi} = 1/k_{20} + k_{-20}[\text{H}_3\text{O}^+]/k_{20}k_{21}$. The plot of $[\text{Fe}^{3+}]/k_{\psi}$ against $[\text{H}_3\text{O}^+]$ for the $\text{L}^1\text{CoOOH}^{2+}/\text{Fe}^{3+}$ reaction is linear and gives a slope of 2.15 ± 0.08 and an intercept of 0.033 ± 0.031 .

(34) (a) Evans, M. G.; George, P.; Uri, N. *Trans. Faraday Soc.* **1949**, *45*, 236. (b) Hagggett, M. L.; Jones, P.; Wynne-Jones, W. F. K. *Discuss. Faraday Soc.* **1960**, *29*, 153.

(35) (a) Liebafsky, H. A.; Mohammed, A. *J. Am. Chem. Soc.* **1933**, *55*, 3977. (b) Wilson, I. R.; Harris, G. M. *J. Am. Chem. Soc.* **1960**, *82*, 4515. (c) Caldwell, S. M.; Norris, A. R. *Inorg. Chem.* **1968**, *7*, 1667. (d) Dankleff, M.; Curci, R.; Edwards, J. O.; Pyun, H. Y. *J. Am. Chem. Soc.* **1968**, *90*, 3209.

(36) Edwards, J. O. *J. Phys. Chem.* **1952**, *56*, 279.

(37) (a) Adzami, I. K.; Libson, K.; Lydon, J. D.; Elder, R. C.; Deutsch, E. *Inorg. Chem.* **1979**, *18*, 303. (b) Adzami, I. K.; Deutsch, E. *Inorg. Chem.* **1980**, *19*, 1366.